Published Paper available here: https://doi.org/10.1016/j.polymertesting.2015.07.007

Ben Alcock, Thijs A. Peters, Rune H. Gaarder, Jens Kjær Jørgensen. *The effect of hydrocarbon ageing on the mechanical properties, apparent crosslink density and CO2 diffusion of a hydrogenated nitrile butadiene rubber (HNBR).* Polymer Testing, Volume 47, 2015, Pages 22-29

The effect of hydrocarbon ageing on the mechanical properties, apparent crosslink density and CO_2 diffusion of a hydrogenated nitrile butadiene rubber (HNBR)

Ben Alcock, Thijs A. Peters, Rune H. Gaarder, Jens Kjær Jørgensen

Abstract

The effect of ageing in a sweet oil environment on the tensile properties, apparent crosslink density, CO2 diffusion and shore hardness of a typical carbon black reinforced hydrogenated nitrile butadiene rubber (HNBR) is presented. Different ageing conditions yielded materials with different properties, attributed to varying degrees of apparent crosslinking. These results showed that, with increasing apparent crosslink density, tensile stiffness and hardness increased, while CO_2 diffusivity and saturation swelling in chloroform decreased. The relationships between these properties suggests that geometry independent tests (such as solvent swelling) may be performed on parts retrieved from service in order to predict properties (such as tensile stiffness or gas diffusion) which cannot normally be measured on retrieved parts due to geometrical constraints.

1. Introduction

The chemical and thermal resistance of hydrogenated nitrile butadiene rubbers (HNBRs) mean that they are often used in sealing applications, particularly in oil and gas distribution. The mechanical, thermal and chemical resistance properties of elastomers in general, can be tailored to suit the application by selecting suitable base chemistries, incorporating various additives and fillers [1-8] and (for crosslinked elastomers) by applying appropriate curing processes [9, 10]. While some general statements can be made about the relationships between composition and performance of polymer products, it is difficult to predict behaviour in real applications which experience complex mechanical loads in aggressive chemical environments.

Since there is extensive history of the use of HNBR seals in aggressive subsea oil and gas applications, there is a huge number of HNBR sealing parts which are periodically removed during routine maintenance and, due to their low replacement cost and the time constraints during maintenance operations, immediately discarded. While chemical analysis of these

parts can be performed, it is difficult to extract useful mechanical information from the seals due to the fact that seal geometries are not well suited to conventional mechanical testing and the seals are often damaged on removal. Such mechanical information would be valuable to validate the predictions of accelerated ageing studies commonly performed on tensile specimens in laboratories during material development.

The focus of this paper is to present the relationships between parameters which require specific geometries for measurement (such as tensile stiffness and diffusion characteristics) with parameters that require much more simple geometries (Shore hardness) or are largely independent of geometry (crosslink density). Previous work by the same authors has shown that an aggressive chemical environment at elevated temperature and pressure can be used in the laboratory to age HNBR specimens [11], and the main mechanism active in the ageing of HNBR appears to be an increase in the apparent crosslink density. In a continuation of that study, HNBR specimens which have been aged to varying degrees are now subjected to further analyses to determine the relationship between the stiffness measurements (which require a specific test geometry and, therefore, cannot be easily applied to retrieved seals) and saturation solvent swelling tests (which do not require specific test geometries and so could be applied to any retrieved parts). Additionally, as an alternative mechanical measure, hardness measurements are performed on aged specimens to investigate the relationship between the hardness and tensile stiffness of aged HNBR parts. Finally, the gas diffusion properties (which, like tensile measurements, also require a large, defect free test geometry and, therefore, not easily applicable to retrieved seals) are also investigated to show the relationship between gas permeation and apparent crosslink density. In principle, such relationships would allow the estimation of mechanical properties and gas diffusion characteristics from seals retrieved from service, only by performing only a solvent swelling test.

The results presented in this paper are from experimental techniques which may be applied quickly and cheaply, without the need for very specialized analysis equipment, in order that they may be applied as widely as possible. However, more advanced techniques to characterise rubber exist such as atomic force microscopy (AFM) [12-14] to quantify surface stiffness or nuclear magnetic resonance (NMR) spectroscopy to describe crosslink density [15-18] although such methods do require rather specialised equipment. The well-known Mooney-Rivlin equation could also be applied to calculate the crosslink density of filled elastomers from mechanical data [19], although this also requires specific test geometries and is difficult to apply to seals. In reality, it is rather complex to accurately determine the crosslink density of a cured elastomer [20], especially one which is filled with particulate reinforcements such as carbon black [21]. However, calculation of the real crosslink density may not be necessary for the kind of correlations with mechanical data presented here. Of more practical use is a quick and simple measure attained using solvent swelling, which in this paper is termed the *apparent* crosslink density, and is discussed later. This apparent crosslink density may be readily measured using only very basic equipment, and can be used to estimate the

mechanical properties of a complex part, based on prior knowledge of the relationship between crosslink density and stiffness. Although compression set was not considered in the work presented here, a similar correlation between compression set and crosslink density of air aged NBR specimens has been reported previously by Morrell *et al.* [22].

Specifically, the solvent swelling and CO_2 diffusion characteristics of HNBR following ageing in an oil simulating chemical environment under elevated temperature and pressure are presented in this paper. In addition, the apparent crosslink densities of HNBRs in a virgin state (i.e. as prepared), or after the chemical ageing, are calculated based on saturated swelling of the HNBRs in an appropriate solvent. The Shore D hardness is also presented as a further indicator of how the mechanical properties change due to the chemical ageing of the HNBR.

2. Experimental

2.1. Materials

HNBR was compounded as summarised in Table 1, using a base polymer which is 96% saturated with 36% acrylonitrile content. The HNBR was cured in a hot press for 20minutes at 170°C and then 4 hours at 150°C in a hot air oven to yield 2mm thick sheets from which test pieces were subsequently produced. The inclusion of 50phr HAF N-330 carbon black (26-30nm primary particle diameter [23]), yields a weight fraction of carbon black of 27% .

Table 1. Composition of the HNBR assessed in this paper.

Material	phr
HNBR	100
Antioxidant	3
Stearic acid	0.5
Zinc Oxide	5
Magnesium Oxide	10
N-330 HAF Carbon Black	50
Plasticizer	20
Peroxide	10

2.2. Chemical Exposure (Ageing)

The procedure of exposure of HNBR samples to organic solvents at elevated temperature and pressure has been described in detail in a previous publication [11], but will be summarized here for completeness. The HNBR samples were placed in a hydrocarbon liquid phase (variation classification A.1.ii) with a gas phase (variation classification A.2.i), as suggested by ISO 23936-2:2011 Annex A, and as summarised here in Table 2. Specimens were held in a series of purpose built titanium frames located inside the organic liquid phase (which is immiscible with the aqueous phase) inside one of numerous titanium pressure vessels. The pressure was raised to 100bar (~1450psi) at set temperatures for different time periods, as

summarised in Table 3. Each pressure vessel was maintained at a single temperature during the exposure time. Different time periods were achieved by depressurizing and removing some specimens from each pressure vessel at various time points, and then re-pressurizing the pressure vessels with the remaining specimens inside.

Table 2. Chemical environment for exposure of specimens.

Proportion of Total Volume	Proportion of Phase
30% gas	95% CH_4
	5% CO_2
10% De-ionised water	-
60% organic liquid ("Test Solvent Mix")	70% Heptane
	20% Cyclohexane
	10% Toluene

Table 3. Specimen names to identify exposure conditions included in this study. All specimens were included in swelling and hardness testing. [(a)] Indicates specimens also included in diffusion testing.

Ageing Time / Ageing Temperature	3 Weeks	6 Weeks	12 Weeks
130°C	-	-	130°C, 12w
140°C	-	140°C, 6w[(a)]	140°C, 12w
150°C	150°C, 3w	150°C, 6w	150°C, 12w
160°C	160°C, 3w	160°C, 6w[(a)]	160°C, 12w[(a)]

2.3. Test Methods

2.3.1. Swelling Behaviour of HNBR in Various Organic Solvents

The swelling ratio of various specimens was assessed as a means of measuring the apparent crosslink density of the specimens [24]. The Hildebrand solubility parameters of the solvents reported here are listed in Table 4. HNBR specimens were cut from virgin and exposed tensile specimens, to give swelling specimens with a mass of 0.2±0.05g; a minimum of four replicates of each specimen was tested. The specimens were immersed in an excess of solvent (typically 0.2cm^3 of HNBR in 50ml of liquid), and removed periodically, surface dried with a tissue, immediately weighed on a microbalance and then returned to the solvent. Post-ageing swelling tests were performed by swelling at ambient temperature and pressure. The immersion of the swelling specimens in solvent was continued until a saturation weight had been achieved (typically within 72 hours, but verified experimentally up to 6 months later). The mass swelling percentage (Q) were calculated as shown in Equation 1 [25]:

Equation 1

$$Q = \frac{W_s - W_d}{W_d} \times 100$$

where W_s is the weight of the saturated specimen and W_d is the weight of the dry specimen. All specimens were produced from the same original batch of material and, therefore, assumed to have uniform composition and distribution of filler (i.e. carbon black). It is also assumed that the non-HNBR component of the compound (i.e. carbon black, magnesium oxide etc.; see Table 1) to be inert with respect to swelling behaviour. Although magnesium oxide is reported to yield swelling effects due to hydration in HNBR [26], the 10phr MgO present in this formulation (see Table 1), equivalent to a weight fraction of ca. 5% (volume fraction of ca. 2%) is uniform for all specimens and ignored in the swelling calculations presented here.

2.3.2. Shore Hardness

The Shore D hardness measurement was performed on a selection of the materials indicated by (a) in Table 3. The samples were measured using a Bareiss automated durometer hardness tester, following ISO 7619-1. The measurements represent the hardness at a 3 second test time. The measurement of hardness on samples which are ca. 2mm thick is a significant deviation from the guidance of ISO 7619-1. The dimensions of the sample are known to influence the hardness measurement and, while the hardness values presented here are for samples of this thickness (ca. 2mm), these would differ from measurements performed on thicker (>6mm) specimens, since the measured hardnesses of relatively thin, soft specimens are influenced by the platform holding the specimen. Therefore, the hardness values presented here should be considered to be relative rather than absolute. Although HNBR compounds are normally specified in the Shore A scale, the initial starting material was approximately Shore 90A. Considering that the accuracy of the Shore hardness scales decreases when measuring above 90 or below 10 [27], and the hardness of the HNBR was expected to increase as a result of the ageing in the chemical environment, the materials were characterized in the Shore D scale instead.

2.3.3. CO_2 Permeability through HNBR

In order to assess any changes in permeability of gases through HNBR, CO_2 was selected as a model gas. Selected HNBR sheets (indicated by (b) in Table 3) which had previously been exposed to different temperatures and durations in the chemical environment described earlier, were placed in a stainless steel high-pressure diffusion cell. The test samples had an area of approximately 50cm^2 (dimensions 50 x 100mm), although the area of the sample which is open to a porous support (24cm^2) is used in the calculation of the permeability. It is assumed that the porous support does not affect the gas flow through the sample, and no leakage around the specimen occurs.

Automated mass flow controllers (Bronkhorst High-Tech) were used to control the gas supply to the feed of the HNBR sheet. The temperature profile of the cell with time is shown schematically in Figure 1. The module was heated to 80°C, with the sample in a N_2/Ar (99.999%) atmosphere until 80°C was reached, at which point the N_2 was replaced with CO_2 (99.95%) and the pressure increased to 3 bars. The pressure of the feed side of the HNBR sheet was controlled with the help of a back pressure controller (Bronkhorst High-Tech). The volume below the HNBR sheet was flushed at a constant flow rate of argon at atmospheric pressure via a mass flow controller (Bronkhorst High-Tech) in order to remove the permeated gases from the HNBR sheet. The CO_2 permeation flux was calculated from the measured CO_2 concentration in the permeate using the calibrated flow of argon sweep gas. For this, the permeate composition was monitored by a gas chromatograph (Varian Inc., CP-4900) equipped with a thermal conductivity detector (TCD). CO_2 flux measurements have been performed applying a feed pressure 20 bars, at temperatures of 80, 60 and 40°C, as shown schematically in Figure 1. After changing the temperature, the CO_2 flux was left to stabilize isothermally for 2-3 days to ensure appropriate measurement. These isothermal steps are used to measure the steady state permeability, *P*, at different temperatures while the initial breakthough of the CO_2 at 80°C allows measurement of the diffusivity, *D*. Combining these according to Equation 2 allows the calculation of the solubility, *S*. It is assumed that this additional 6-9 days at 40-80°C does not further influence the characteristics of the HNBR, as it is not considered significant compared to the previous 12 week ageing at 140 or 160°C.

Equation 2

$$S = \frac{P}{D}$$

Figure 1*. Schematic of temperature profile during permeability measurements. The relative pressure on the feed side of the cell is increased, and (a) the temperature is raised from ambient temperature to the first temperature level (80°C), at which point an isothermal step is held (b) to measure the permeability. The sample temperature is then reduced to subsequent isothermal steps 60°C (c) and 40°C (d) to capture permeability measurements at each of the different temperatures.*

3. Results and Discussion

3.1. Swelling of HNBR in Solvents

3.1.1. Swelling of virgin HNBR in various test solvents

In order to confirm the most suitable solvent to exaggerate the saturation swelling of HNBR, virgin HNBR specimens (i.e. HNBR specimens of the same composition as shown in Table 1, but which had not be subjected to any ageing treatment) were saturated by immersion in the following solvents: heptane, cyclohexane, toluene, chloroform, acetone and a 7:2:1 volumetric mix of heptane, cyclohexane and toluenewhich is the test solvent mix used in the ageing exposure. The saturation degree of swelling of virgin HNBR in these solvents is shown

in Figure 2. The solubility parameters reported in literature for each of these solvents, and a calculated solubility parameter for the test solvent mix, are shown in Table 4.

Table 4. Solvents and Hildebrand solubility parameters applied in this research [28], together with saturation swelling of the virgin (unaged) HNBR compound in these solvents.

Solvent	Hildebrand Solubility Parameter ($MPa^{1/2}$)	Saturation Swelling (%)
Acetone	20.3	50.57
Chloroform	19.0	249.12
Toluene	18.2	67.08
Cyclohexane	16.8	11.17
Heptane	15.1	5.25
Test Solvent Mix: Heptane, cyclohexane, toluene (7:2:1) mix	15.75*	10.69

*Solubility parameter for the heptane, cyclohexane, toluene mix was calculated by proportioning individual solvent parameters.

Figure 2. *Saturated swelling (measured by mass increase) of virgin HNBR in various solvents. The test solvent mix identified in this graph is the heptane:cyclohexane:toluene (7:2:1) mix used for ageing in pressure vessels.*

Figure 2 suggests that the solubility parameter for this HNBR is between the solubility parameters of toluene and acetone (18.2-20.3$MPa^{0.5}$). In this work, it is assumed the solubility parameter of the HNBR used here is 19.2$MPa^{0.5}$, i.e. the midpoint of the range mentioned and well within the range reported in literature for similar HNBRs (17.8-20.69$MPa^{0.5}$[29], 17.9 $MPa^{0.5}$[30], 19.7$MPa^{0.5}$[31] and 19.9$MPa^{0.5}$[32, 33]). Of the solvents investigated here, it is clear that chloroform gives the highest saturation swelling for the HNBR, and the test solvent mix does not give a very strong swelling of this HNBR. It is interesting to note that the test solvent mix leads to a saturation swelling in ambient pressure and temperature of 10.7% (from Table 4), while exposure to the same solvent environment at elevated temperature and pressure was previously shown to yield a higher saturation swelling of at least 14% [11] when exposed in pressure vessels at elevated temperature and 100bar of pressure.

3.1.2. Swelling of aged materials in Chloroform

The swelling of aged HNBRs in chloroform was measured with a maximum (saturation) swelling achieved after approximately 24 hours, although the specimens were also weighed after several months to confirm the saturation was stable. Chloroform was selected since Figure 2 showed that of the solvents considered chloroform gave the greatest swelling of HNBR. The mass uptake over time in chloroform for selected (previously aged specimens) is shown in Figure 3. The total mass increase due to chloroform uptake for a wider range of specimens is shown in Figure 4. The results clearly show that increased ageing decreases later

mass uptake due to swelling in chloroform, and the lowest saturated swelling in chloroform occurs following the combined highest ageing temperature and longest ageing time in the test solvent mix.

Figure 3. *Chloroform uptake of selected (previously) aged specimens. Note that as ageing time and temperature increases, mass gain due to chloroform absorption decreases.*

Figure 4. *Mass increase due to saturated swelling in chloroform at ambient conditions of samples previously aged in the test solvent mix. Lines join data points of equal ageing time. The horizontal dotted line represents the saturated swelling of the virgin HNBR.*

The degree of saturated swelling is frequently reported to approximate the apparent degree of crosslinking in rubbers; a reduction in saturated swelling of a rubbery material in a suitable solvent is associated with an increase in crosslink density [9, 22, 24, 25, 33-38]. In principle, the molecular weight between crosslinks, M_c, can be determined from the network density of crosslinking, v_c, from **Equation 3** and **Equation 4**, in which V_S is the molecular volume of the solvent (80.66cm^3.mol^{-1} for chloroform), V_R is volume fraction of polymer in the swollen state calculated from **Equation 5**. χ is an interaction parameter between the solvent and the polymer, as defined in **Equation 6**, in which δ_s and δ_r are the solubility parameters for chloroform (19MPa$^{0.5}$[39]) and polymer (estimated from to be 19.3MPa$^{0.5}$) respectively, and R and T are the universal gas constant (8.314 J.mol^{-1}.K^{-1}) and absolute temperature (293K) respectively. Since δ_s and δ_r are similar in value, χ is very small and so does not greatly influence the relative calculation of v_c for different specimens. Therefore, the exact values of δ_s and δ_r are not critical for a first approximation [25].

Equation 3

$$v_c = \frac{1}{V_s}\left(\frac{\ln(1-V_R)+V_R+\chi {V_R}^2}{\left(\frac{V_R}{2}-{V_R}^{1/3}\right)}\right)$$

Equation 4

$$M_c = \frac{\rho}{v_c}$$

Equation 5

$$\boldsymbol{V_R = \frac{\left(W_p/\rho_p\right)}{\left(W_p/\rho_p\right)+\left(W_{CB}/\rho_{CB}\right)+\left(W_s/\rho_s\right)}}$$

where V_R is the volume fraction of polymer in the swollen material, W_p, W_{CB} and W_S are the weight fractions of polymer, carbon black and solvent, respectively, in the swollen material, and ρ_p, ρ_{CB} and ρ_S are the densities of the polymer, carbon black and solvent, respectively. It

is assumed that the density of the polymer component ρ_p is constant for all specimens and affected by neither ageing nor changes in apparent crosslink density.

Equation 6

$$\chi = \frac{(\delta_s - \delta_r)^2 V_s}{RT}$$

Applying **Equation 3** to the results presented in Figure 4, allows a similar graph to be created to show the apparent crosslink density, M_c, (the apparent molecular weight between crosslinks), and this is presented in Figure 5. The results in Figure 4 suggest a 3.2x decrease in chloroform saturation swelling when comparing the most aged specimens (160°C, 12w) with the virgin specimens. Figure 5 shows an approximate 2.5x increase in apparent crosslink density of the most aged specimens compared to virgin HNBR specimens.

Figure 5. *Apparent molecular weight between crosslinks of samples previously aged in the test solvent mix. Lines join data points of equal ageing time. The horizontal dotted line represents the apparent molecular weight between crosslinks in the virgin HNBR.*

It should be considered that the measurement of M_c presented here is an oversimplification of the real situation in a number of ways. Firstly, the swollen material is modelled as a three phase system comprising a polymer, carbon black and absorbed solvent (see **Equation 5**). In reality, Table 1 shows that the material comprises a large number of ingredients, some of which (such as zinc oxide) will probably act rather like large inert fillers within the polymer matrix and, therefore, probably do not contribute positively to solvent absorption. Other ingredients, such as the commercial peroxide product used here also comprise large amounts of inorganic filler. Additionally, there is the possibility that some uncrosslinked groups dissolve out the specimens during swelling, although this should only affect the virgin specimens as for the previously aged specimens, any leaching would be expected to have already occurred during previous ageing. These uncertainties regarding exact composition of the cured compound lead to underestimating the solvent absorption per unit mass of polymer and, therefore, overestimating M_c. Secondly, the presence of reinforcing fillers can greatly reduce local molecular mobility and, therefore, can act in the same way as chemical crosslinks to impede the three dimensional deformation required for swelling to occur [23, 40, 41]. This could lead to an overestimation of the crosslink density. Thirdly, it is assumed that the polymer itself does not change density as a function of crosslink density or ageing. An increase in density which could result from increasing crosslinking would be expected to lead to a decrease in calculated M_c Therefore, underestimating the polymer density leads to overestimating M_c. Considering these factors, M_c is referred to here as an *apparent* crosslink density, useful for comparing materials of the same composition (considering the limitations described above) but not intended to accurately describe the real situation regarding actual chemical crosslinks in this complex material [20].

Figure 6 shows the relationship between the saturation swelling shown in Figure 3, and tensile modulus results of these specimens (after drying), as presented previously [11], while Figure 7 shows the relationship between apparent crosslink density as calculated using **Equation 4**. A trendline shows that the log of the tensile modulus and saturation swelling or apparent crosslink density of these specimens follow linear behaviour on these axes. This relationship is particularly valuable as it suggests that the tensile modulus of HNBR samples could be predicted by saturation swelling tests, even when the samples are not available in a form suitable for mechanical testing (such as o-rings or more complex geometries). For practical use in an industrial environment, the saturation swelling data shown in Figure 6 is probably more useful than the calculation of apparent crosslink density shown in Figure 7, as it does not require additional density calculations that can influence the result of **Equation 3**. In order to only compare specimens which have been exposed to the test solvent mix, the virgin specimens were not included in the creation of the trendline, although they do not deviate greatly from it.

Figure 6. *Chloroform uptake of selected (previously) aged specimens as a function of tensile modulus. The dotted line represents a linear fit (R^2=0.982, virgin material is excluded from fit).*

Figure 7. *Calculated apparent crosslink density of selected (previously) aged specimens as a function of tensile modulus (based on data presented in Figure 3, and applying Equation 3). The dotted line represents a linear fit (R^2=0.991, virgin material is excluded from fit).*

3.2. Shore D Hardness

The Shore D hardness of selected specimens after removal from the ageing exposure and subsequently dried in air is presented in Figure 8. It is clear that the hardness also increases with increasing time and temperature of exposure to the test solvent mix. The Shore D hardness of the virgin material is shown as the lower solid horizontal line in Figure 8. By plotting the Shore D hardness against the log of the tensile modulus, as presented previously [11], a relationship can be observed, as illustrated by the trendline in Figure 9. This relationship between the log of E and Shore D hardness agrees with work presented elsewhere [27], and shows that the Shore D hardness may be used as a predictor of tensile modulus, although unlike the saturation swelling results shown in Figure 6, the Shore D hardness measurement is affected by specimen geometry so may not be as readily performed on complex geometries as saturation swelling tests.

Figure 8. *Shore D hardness vs. ageing exposure time. The Shore D hardness of the virgin material is represented by a horizontal solid line (with dashed lines representing the standard deviation of the virgin materials).*

Figure 9. *Shore D hardness of selected (previously) aged specimens as a function of tensile modulus. The dotted line represents a linear fit (R^2=0.973, virgin material is excluded from fit).*

3.3. Diffusion of CO_2 through HNBR

The changes seen in the apparent crosslink density as a function of exposure conditions would be expected to influence the ability of liquids and gases to permeate through the materials. The change in permeability of selected HNBR sheets following ageing is shown in Figure 10. As would be expected, higher experimental temperatures lead to higher permeability for all specimens. A decrease in permeability to CO_2 is seen with increasing ageing time at 160°C. Also included here is a specimen which has been aged for 12 weeks at 140°C. This demonstrates that the change in permeability is a function of ageing time as well as temperature, and the relationship seems to fit with apparent crosslink density rather than only for specimens aged at 160°C. Figure 11 shows the relationship between the CO_2 permeability of HNBR to the calculated molecular weight between crosslinks. Linear trendlines are fitted to the data with extrapolation through zero permeability, showing that for each diffusion temperature considered here (40, 60 and 80°C), the data for all the specimens have an excellent fit, confirming that the permeability to CO_2 is closely related to the apparent crosslink density derived from the maximum saturation swelling in solvents (shown in Figure 4).

Figure 10. *CO_2 permeability as a function of ageing time, showing a decrease in permeability with increasing ageing time for the specimens aged at 160°C (closed symbols). Also included is a specimen aged at 140°C for 12 weeks (open symbol), showing that specimens aged at 140°C show greater permeability than those aged at 160°C for the same duration.*

Figure 11. *CO_2 permeability of HNBR sheets as a function of the apparent molecular weight between crosslinks. Linear trendlines for each diffusion temperature group (40, 60 and 80°C) are fitted through the origin (R^2>0.996 in each case). As in Figure 10, a specimen aged at 140°C for 12 weeks is included, showing that specimens aged at 140°C (open symbols) show greater permeability than those aged at 160°C (closed symbols) for the same duration.*

The diffusivity of the specimens at 80°C was also measured and is shown in Figure 12. The measurement of diffusivity and permeability allows the calculation of the solubility, which is also shown in Figure 12. This shows that the diffusivity and permeability, and thus also the solubility, decrease with increasing apparent crosslink density of these HNBR specimens, meaning that the barriers properties of HNBR would be expected to increase with time in service. This increased barrier property is positive for sealing applications, but the reduced permeability also leads to greater risk of rapid gas decompression (RGD) damage. RGD damage is caused as dissolved gas enters the material during pressurization but cannot dissolve out quickly enough during rapid depressurization, resulting in structural damage (crack formation) within the material. Therefore, the diffusivity performance of HNBR is very relevant to subsea applications which may be subjected to pressure fluctuations during service.

Figure 12*. The diffusivity and solubility of HNBR sheets as a function of the apparent molecular weight between crosslinks.*

4. Conclusions

An HNBR compound which had been previously aged to varying degrees and, therefore, possesses a range of apparent crosslink densities, has been investigated here. Clear relationships have been observed between the apparent crosslink density of small specimens and tensile stiffness, Shore hardness and CO_2 permeability of larger specimens.

The use of simple saturation swelling tests has been shown to yield data from very small amounts of material which may then be used to predict the stiffness or gas permeability of the materials from predetermined relationships. Due to the unsuitable geometry of retrieved parts, direct stiffness or diffusion measurements would be difficult or impossible to measure directly. Therefore, it is expected that such an approach could be a simple and effective method to estimate the characteristics of HNBR specimens retrieved from service. Since there are currently large numbers of standard HNBR products in service, the collection and assessment of end-of-life parts following replacement during routine maintenance could allow a greater understanding of real time ageing processes in these materials.

5. Acknowledgements

This work is part of the collaborative project “PolyLife” with the industrial partners FMC Kongsberg Subsea AS, Kongsberg Oil & Gas Technologies AS, Roplast GmbH, Petróleo Brasileiro SA and the research institutes Norwegian University of Science and Technology (NTNU) and SINTEF Materials and Chemistry. The authors would like to express their thanks for the financial support by The Research Council of Norway (Project 193167 in the Petromaks programme).

References

1. Campomizzi, E.C., H. Bender, and W. von Hellens, *Improving the heat resistance of Hydrogenated nitrile rubber compounds. Part 2: Effect of a novel heat stabilizer additive on the heat resistance of HNBR.* Kautschuk Gummi Kunststoffe, 2001. **54**(3): p. 114-121.
2. Chen, S., et al., *Thermal degradation behavior of hydrogenated nitrile-butadiene rubber (HNBR)/clay nanocomposite and HNBR/clay/carbon nanotubes nanocomposites.* Thermochimica Acta, 2009. **491**(1): p. 103-108.
3. Mohan, T.P., J. Kuriakose, and K. Kanny, *Effect of nanoclay reinforcement on structure, thermal and mechanical properties of natural rubber–styrene butadiene rubber (NR–SBR).* Journal of Industrial and Engineering Chemistry, 2011. **17**(2): p. 264-270.
4. Mohan, T.P., J. Kuriakose, and K. Kanny, *Water uptake and mechanical properties of natural rubber–styrene butadine rubber (nr-sr) – Nanoclay composites.* Journal of Industrial and Engineering Chemistry, 2012. **18**(3): p. 979-985.
5. Gatos, K.G., et al., *Nanocomposite Formation in Hydrogenated Nitrile Rubber (HNBR)/Organo-Montmorillonite as a Function of the Intercalant Type.* Macromolecular Materials and Engineering, 2004. **289**(12): p. 1079-1086.
6. Cadambi, R.M. and E. Ghassemieh, *The ageing behaviour of hydrogenated nitrile butadiene rubber/nanoclay nanocomposites in various mediums.* Journal of Elastomers and Plastics, 2012. **44**(4): p. 353-367.
7. Choudhury, A., et al., *Effect of Various Nanofillers on Thermal Stability and Degradation Kinetics of Polymer Nanocomposites.* Journal of Nanoscience and Nanotechnology, 2010. **10**(8): p. 5056-5071.
8. Thavamani, P., et al., *The effect of crosslink density, curing system, filler and resin on the decomposition of hydrogenated nitrile rubber and its blends.* Thermochimica Acta, 1993. **219**(0): p. 293-304.
9. Osaka, N., M. Kato, and H. Saito, *Mechanical properties and network structure of phenol resin crosslinked hydrogenated acrylonitrile-butadiene rubber.* Journal of Applied Polymer Science, 2013: p. n/a-n/a.
10. Wei, Z., et al., *Dramatic influence of curing temperature on micro–nano structure transform of HNBR filled with zinc dimethacrylate.* Journal of Applied Polymer Science, 2012. **124**(1): p. 288-295.
11. Alcock, B. and J.K. Jørgensen, *The mechanical properties of a model hydrogenated nitrile butadiene rubber (HNBR) following simulated sweet oil exposure at elevated temperature and pressure.* Polymer Testing, 2015. **tbc**(tbc): p. tbc.
12. Tranchida, D., S. Piccarolo, and M. Soliman, *Nanoscale Mechanical Characterization of Polymers by AFM Nanoindentations: Critical Approach to the Elastic Characterization.* Macromolecules, 2006. **39**(13): p. 4547-4556.
13. Ferencz, R., et al., *AFM nanoindentation to determine Young's modulus for different EPDM elastomers.* Polymer Testing, 2012. **31**(3): p. 425-432.
14. Gillen, K.T., E.R. Terrill, and R.M. Winter, *Modulus Mapping of Rubbers Using Micro- and Nano-Indentation Techniques.* Rubber Chemistry and Technology, 2001. **74**(3): p. 428-450.
15. Chae, Y.K., et al., *A simple NMR method to measure crosslink density of natural rubber composite.* Polymer Testing, 2010. **29**(8): p. 953-957.
16. Garbarczyk, M., et al., *Characterization of aged nitrile rubber elastomers by NMR spectroscopy and microimaging.* Polymer, 2002. **43**(11): p. 3169-3172.
17. Kuhn, W., et al., *Characterization of elastomeric materials by NMR-microscopy.* Solid State Nuclear Magnetic Resonance, 1996. **6**(4): p. 295-308.

18. Garbarczyk, M., et al., *A novel approach to the determination of the crosslink density in rubber materials with the dipolar correlation effect in low magnetic fields.* Journal of Polymer Science Part B: Polymer Physics, 2001. **39**(18): p. 2207-2216.
19. Mullins, L. and N.R. Tobin, *Stress softening in rubber vulcanizates. Part I. Use of a strain amplification factor to describe the elastic behavior of filler-reinforced vulcanized rubber.* Journal of Applied Polymer Science, 1965. **9**: p. 2993-3009.
20. Valentín, J.L., et al., *Uncertainties in the Determination of Cross-Link Density by Equilibrium Swelling Experiments in Natural Rubber.* Macromolecules, 2008. **41**(13): p. 4717-4729.
21. Rowlinson, M., et al., *The Effect of Carbon Black Morphological Characteristics on Tear Propagation In Rubbers.* Kautschuk Gummi Kunststoffe, 1999. **12**: p. 830-835.
22. Morrell, P.R., M. Patel, and A.R. Skinner, *Accelerated thermal ageing studies on nitrile rubber O-rings.* Polymer Testing, 2003. **22**(6): p. 651-656.
23. Donnet, J.-B. and E. Custodero, *Reinforcement of Elastomers by Particulate Fillers*, in *The Science and Technology of Rubber*, J.E. Mark, B. Erman, and C.M. Roland, Editors. 2013, Elsevier.
24. Flory, P.J. and J. Rehner, *Statistical Mechanics of Cross-Linked Polymer Networks II. Swelling.* The Journal of Chemical Physics, 1943. **11**(11): p. 521-526.
25. Mousa, A. and J. Karger-Kocsis, *Rheological and Thermodynamical Behavior of Styrene/Butadiene Rubber-Organoclay Nanocomposites.* Macromolecular Materials and Engineering, 2001. **286**(4): p. 260-266.
26. Han, D., et al., *Swellable elastomeric HNBR–MgO composite: Magnesium oxide as a novel swelling and reinforcement filler.* Composites Science and Technology, 2014. **99**(0): p. 52-58.
27. Mix, A.W. and A.J. Giacomin, *Standardized Polymer Durometry.* Journal of Testing and Evaluation, 2011. **39**(4).
28. Grulke, E.A., *Solubility Parameter Values*, in *Polymer Handbook, 3rd Edition*, J. Brandrup and E.H. Immergut, Editors. 1989. p. 519-559.
29. Dikland, H. and M.v. Duin, *A Chemical Modification Approach for Improving the Oil Resistance of Ethylene–Propylene Copolymers*, in *Current Topics in Elastomers Research*, A.K. Bhowmick, Editor. 2008, CRC Press.
30. Choudhury, A., A.K. Bhowmick, and M. Soddemann, *Influence of nanofillers on the sorption and diffusion characteristics of the solvent in vulcanized hydrogenated nitrile rubber nanocomposite.* Journal of Applied Polymer Science, 2013. **128**(4): p. 2556-2562.
31. Campion, R.P. *Model Test 'Oils' Based on Solubility Parameters for Artificial Ageing of Polymers*. in *Polymer Testing '96. The Second International Conference on the Testing of Polymers*. 1996. UK: RAPRA.
32. Liu, G., et al., *A new way to determine the three-dimensional solubility parameters of hydrogenated nitrile rubber and the predictive power.* Polymer Testing, 2013. **32**(6): p. 1128-1134.
33. Liu, G., et al., *Investigation of the swelling response and quantitative prediction for hydrogenated nitrile rubber.* Polymer Testing, 2014. **34**: p. 72-77.
34. Sombatsompop, N., *Investigation of Swelling Behavior of NR Vulcanisates.* Polymer-Plastics Technology and Engineering, 1998. **37**(1): p. 19-39.
35. Perraud, S., et al., *Network characteristics of hydrogenated nitrile butadiene rubber networks obtained by radiation crosslinking by electron beam.* Polymer Degradation and Stability, 2010. **95**(9): p. 1495-1501.
36. Krzemińska, S. and W.M. Rzymski, *Barrierity of hydrogenated butadiene-acrylonitrile rubber and butyl rubber after exposure to organic solvents.* International Journal of Occupational Safety and Ergonomics (JOSE), 2011. **17**(1): p. 41-47.
37. Choi, S.-S. and J.-C. Kim, *Lifetime prediction and thermal aging behaviors of SBR and NBR composites using crosslink density changes.* Journal of Industrial and Engineering Chemistry, 2012. **18**(3): p. 1166-1170.

38. Nandi, S. and H.H. Winter, *Swelling Behavior of Partially Cross-Linked Polymers: A Ternary System.* Macromolecules, 2005. **38**(10): p. 4447-4455.
39. Hansen, C., *Hansen Solubility Parameters: A User's Handbook*. 2007: CRC Press.
40. Bills Jr., K.W. and F.S. Salcedo, *The swelling of unfilled and highly filled polymers.* Rubber Chemistry and Technology, 1962. **35**(2): p. 284-290.
41. Gent, A.N., J.A. Hartwell, and G. Lee, *Effect of Carbon Black on Crosslinking.* Rubber Chemistry and Technology, 2003. **76**(2): p. 517-532.

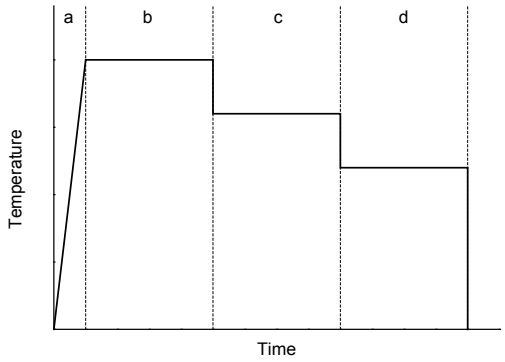

Figure 1. Schematic of temperature profile during permeability measurements. The relative pressure on the feed side of the cell is increased, and (a) the temperature is raised from ambient temperature to the first temperature level (80°C), at which point an isothermal step is held (b) to measure the permeability. The sample temperature is then reduced to subsequent isothermal steps 60°C (c) and 40°C (d) to capture permeability measurements at each of the different temperatures.

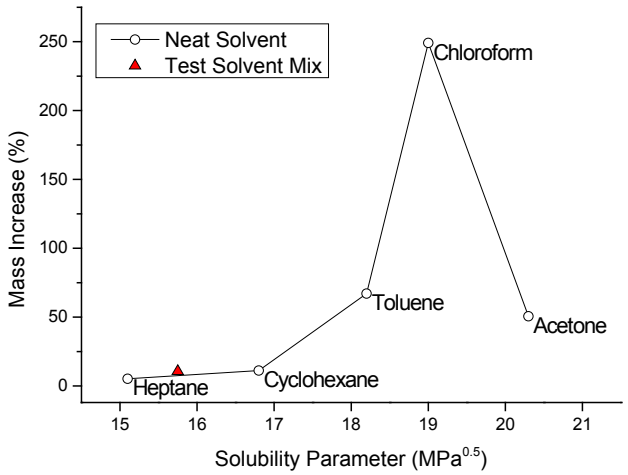

Figure 2. Saturated swelling (measured by mass increase) of virgin HNBR in various solvents. The test solvent mix identified in this graph is the heptane:cyclohexane:toluene (7:2:1) mix used for ageing in pressure vessels.

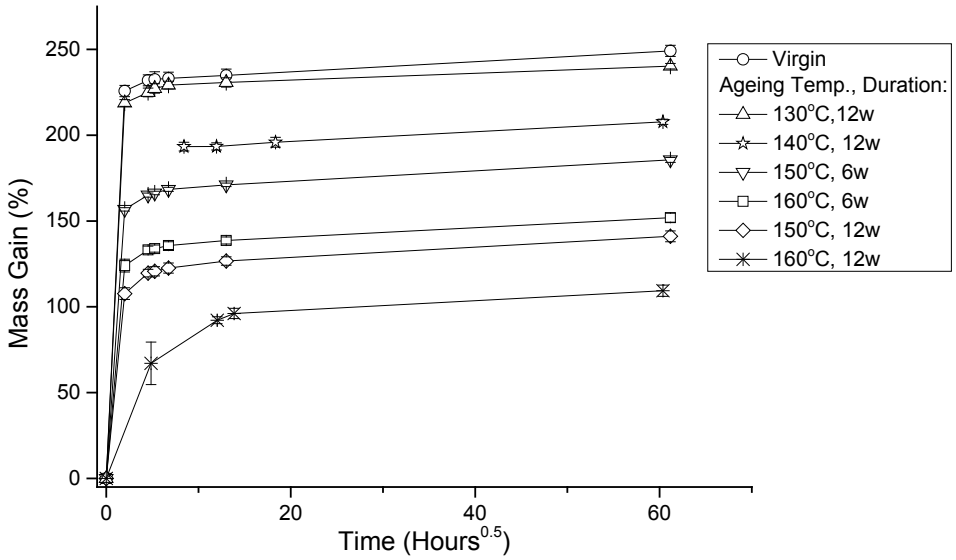

Figure 3. Chloroform uptake of selected (previously) aged specimens. Note that as ageing time and temperature increases, mass gain due to chloroform absorption decreases.

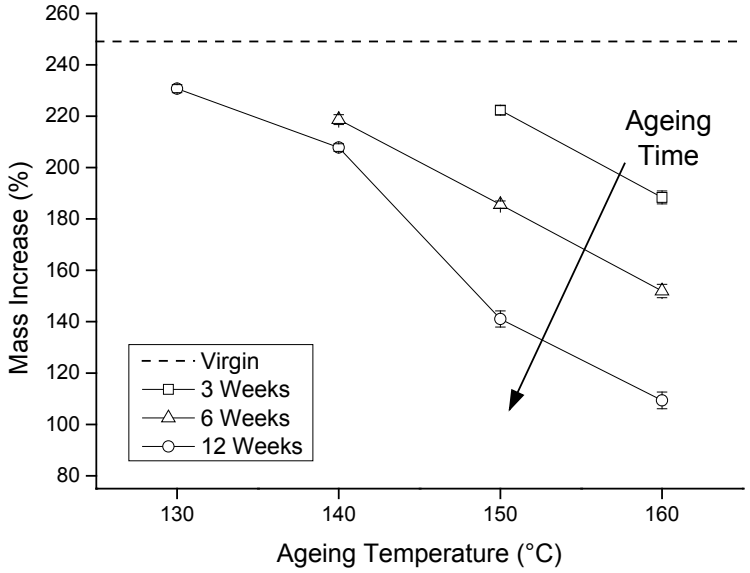

Figure 4. Mass increase due to saturated swelling in chloroform at ambient conditions of samples previously aged in the test solvent mix. Lines join data points of equal ageing time. The horizontal dotted line represents the saturated swelling of the virgin HNBR.

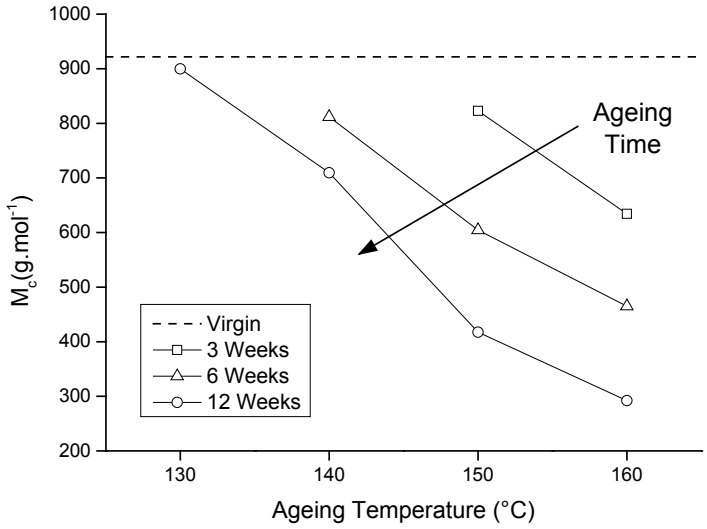

Figure 5. Apparent molecular weight between crosslinks of samples previously aged in the test solvent mix. Lines join data points of equal ageing time. The horizontal dotted line represents the apparent molecular weight between crosslinks in the virgin HNBR.

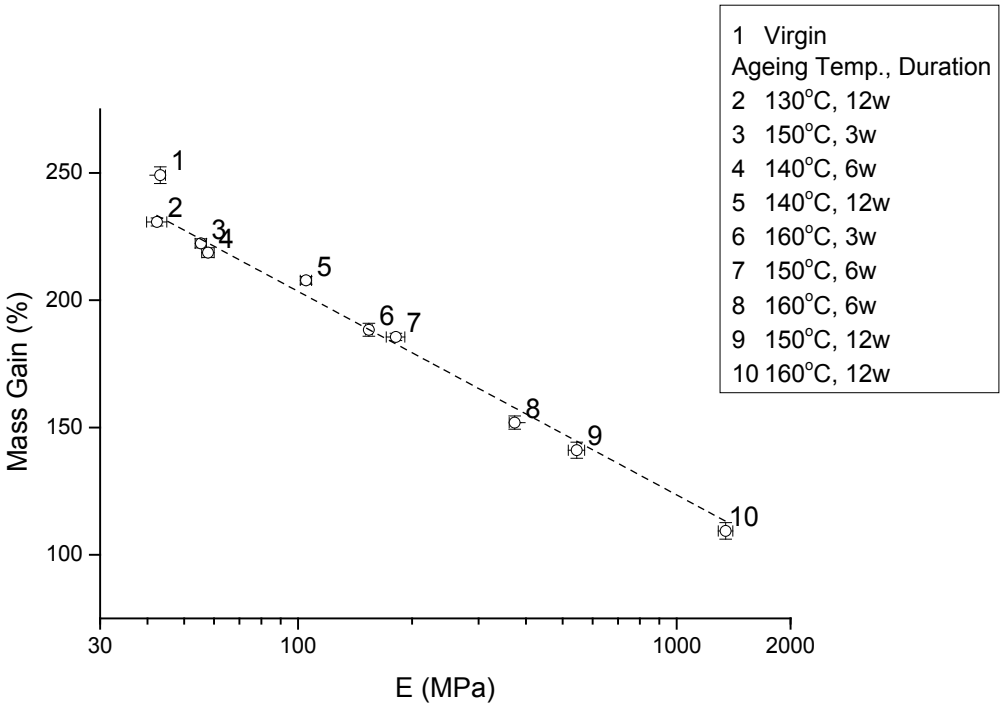

Figure 6. Chloroform uptake of selected (previously) aged specimens as a function of tensile modulus. The dotted line represents a linear fit (R^2=0.982, virgin material is excluded from fit).

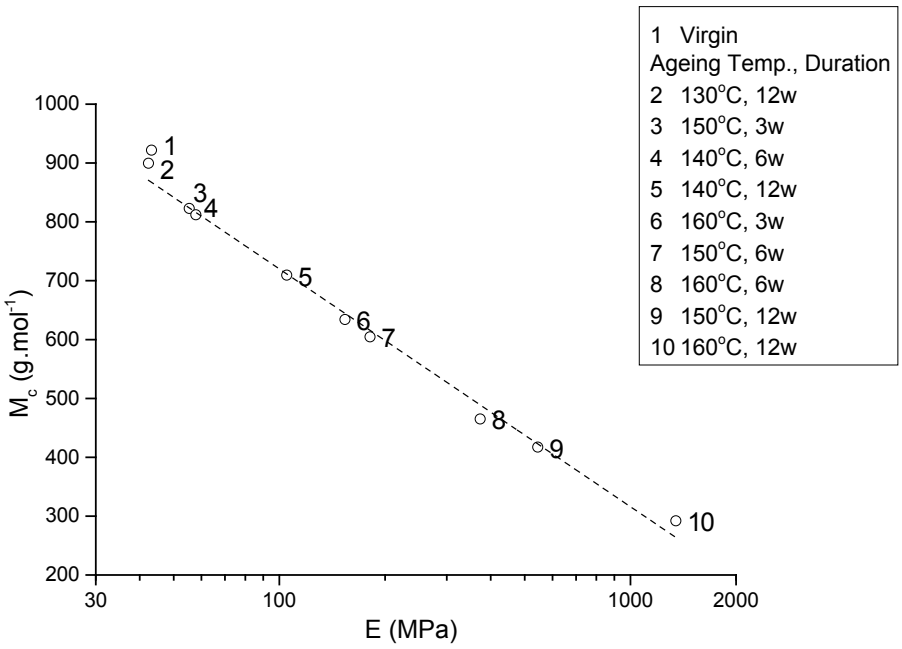

Figure 7. Calculated apparent crosslink density of selected (previously) aged specimens as a function of tensile modulus (based on data presented in **Figure 6**, and applying Equation 3). The dotted line represents a linear fit (R^2=0.991, virgin material is excluded from fit).

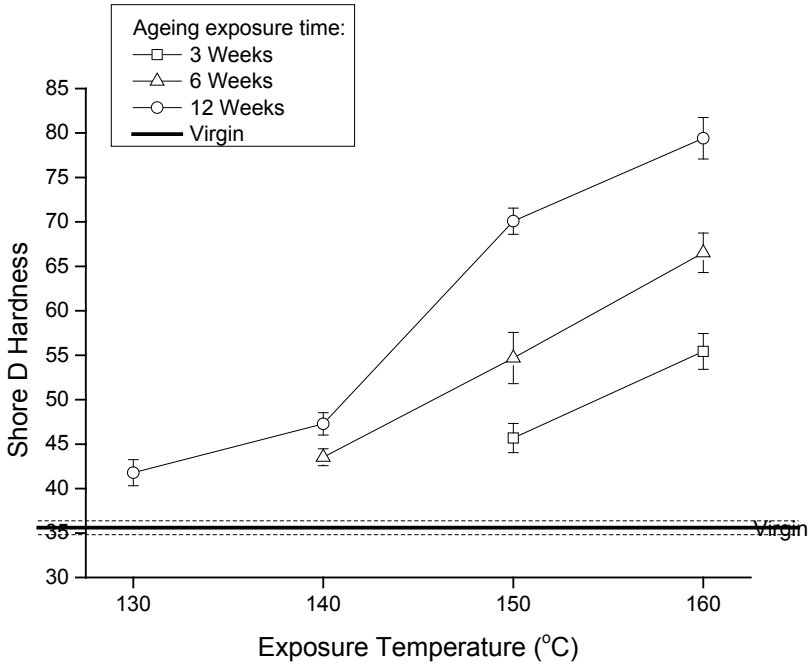

Figure 8. Shore D hardness vs. ageing exposure time. The Shore D hardness of the virgin material is represented by a horizontal solid line (with dashed lines representing the standard deviation of the virgin materials).

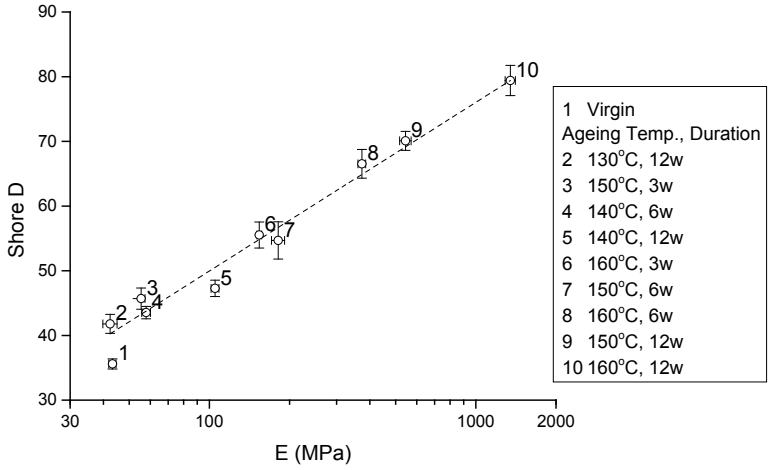

Figure 9. Shore D hardness of selected (previously) aged specimens as a function of tensile modulus. The dotted line represents a linear fit (R^2=0.973, virgin material is excluded from fit).

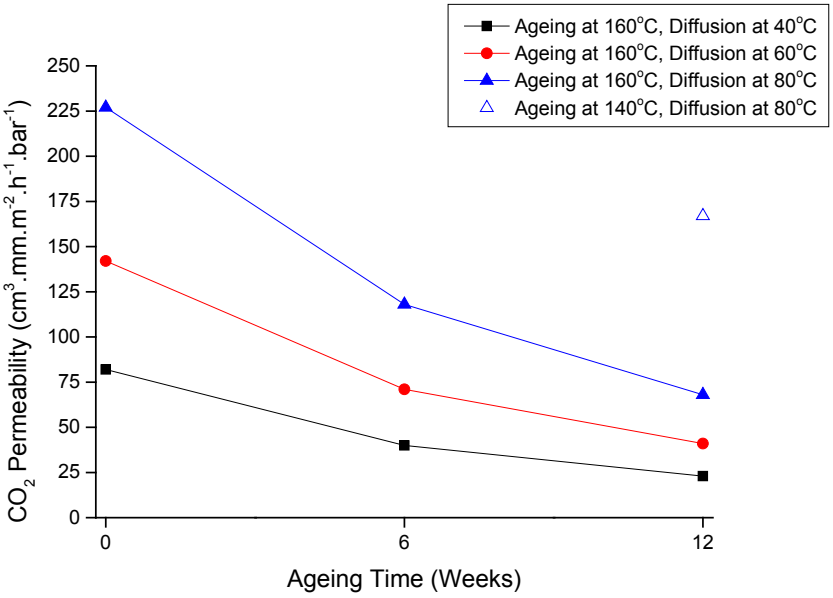

Figure 10. CO_2 permeability as a function of ageing time, showing a decrease in permeability with increasing ageing time for the specimens aged at 160°C (closed symbols). Also included is a specimen aged at 140°C for 12 weeks (open symbol), showing that specimens aged at 140°C show greater permeability than those aged at 160°C for the same duration.

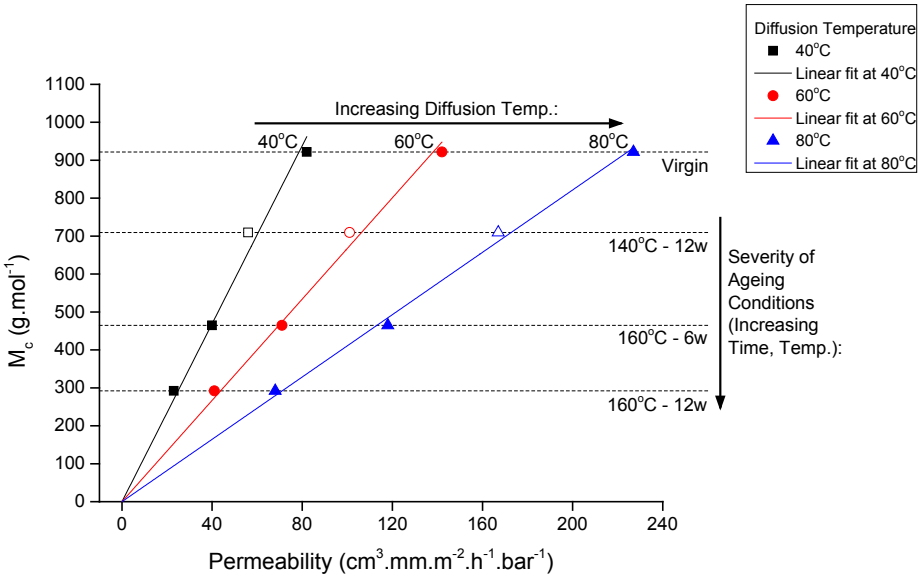

Figure 11. CO_2 permeability of HNBR sheets as a function of the apparent molecular weight between crosslinks. Linear trendlines for each diffusion temperature group (40, 60 and 80°C) are fitted through the origin (R^2>0.996 in each case). As in **Figure 10**, a specimen aged at 140°C for 12 weeks is included, showing that specimens aged at 140°C (open symbols) show greater permeability than those aged at 160°C (closed symbols) for the same duration.

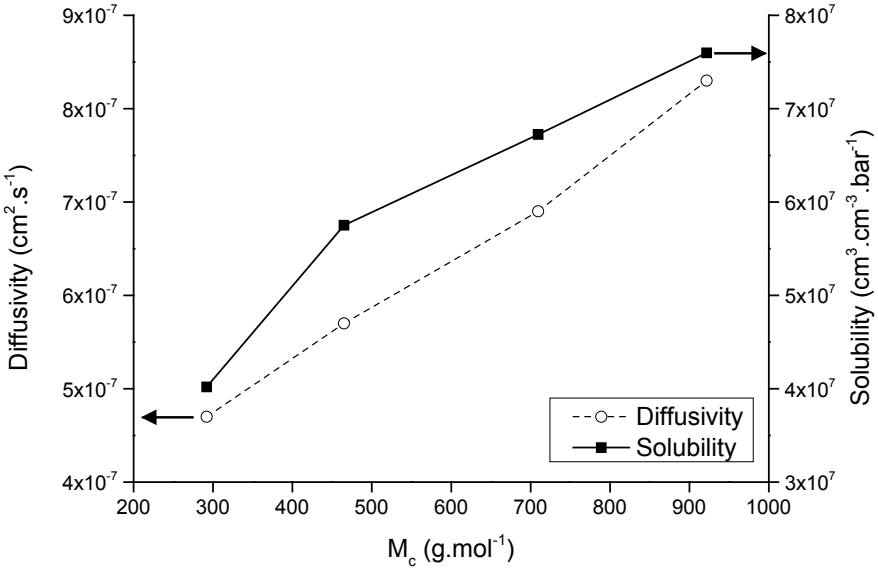

Figure 12. The diffusivity and solubility of HNBR sheets as a function of the apparent molecular weight between crosslinks.